Astron. Astrophys. 226, 288–296 (1989)

ASTRONOMY AND ASTROPHYSICS

The color of the zodiacal light and the size distribution and composition of interplanetary dust

J.-M. Perrin and P.L. Lamy

Laboratoire d'Astronomie Spatiale, Les Trois Lucs, F-13012 Marseille, France

Received March 17, accepted April 18, 1989

Summary. The color of the zodiacal light is studied in the general context of light scattered by dust particles. It is shown that the color is controlled by various mechanisms in a complex way. The spectral variation of the complex index of refraction, the size distribution function and the roughness of the dust grains all play a significant role in the color of the scattered light. It is also shown that the very geometrical conditions of observation of the zodiacal light result in a color effect which depends upon the elongation.

Key words: interplanetary medium – zodiacal light – dust particles

1. Introduction

The brightness of the zodical light observed along a line-of-sight is classically expressed by a double integral, one over the size distribution of the interplanetary grains and the other, over their spatial distribution. Under certain assumptions, it is possible to get rid of this second integral using so-called inversion techniques and to obtain the volume scattering function (VSF) which contains only the integral over the size distribution (Dumont, 1973; Dumont and Sanchez, 1975). This function characterizes the scattering function of a unit volume of interplanetary dust. If the size distribution is assumed independently, one can compute VSF for various types of dust grains and compare with the "observed" function. However, it is well known that such an approach does not really allow to test the size distribution, and that two widely different size distributions can produce similar VSF. Additional observational data are therefore introduced to help disentangling the situation, in particular the color of the zodiacal light. The most recent observations (e.g., Leinert et al., 1982; Cebula and Feldman, 1982) basically indicate a slight reddening from the ultraviolet to the red, but also that this effect depends upon the elongation.

Conventional wisdom leads for instance to conclude that the absence of a blue trend drastically limits the presence of submicronic grains in interplanetary space. The purpose of this work is to show that this symplifying view is not necessarily true and more generally, that the color is controlled by several effects in a complex way; we shall not attempt here to blindly reproduce the observed color of the zodiacal light but rather to explore and understand in which way these various mechanisms determine it. We first define the color ratios of the zodiacal light and of a set of dust grains having a given size distribution function and establish a relationship between the two expressions. We then introduce two different size distributions recently derived; they are viewed here are "extreme" examples in the sense that one favors small grains while the other favors large grains. We then show how the variation of the complex index of refraction with wavelength for real materials modify the classical Rayleigh behaviour; the application of the exact Mie theory combined with the effect of the size distribution may almost annihilate the blue effect even in the case of the distribution emphasizing small grains. We then consider the role of the roughness of the grains and show that the color of the scattered light depends upon the scale of the asperities. In a final section, we prove that the color of the zodiacal light is necessarily a function of elongation in agreement with the above observational results.

2. Expressions of the color of the zodiacal light and of the light scattered by dust grains

2.1. The color of the zodiacal light

Following the assumption and notations used by Lamy and Perrin (1986), the brightness Z of the zodiacal light is given by

$$Z(d, \beta_0, \beta, \varepsilon, \lambda) = F_\odot(\lambda) \frac{d_0^2}{d \sin \varepsilon} \int_\varepsilon^\Pi \psi(\theta, \lambda) R(d, \varepsilon, \theta) \times G(\varepsilon, \beta, \beta_0, \theta) \, d\theta \quad (1)$$

where the geometrical variables and parameters d, β_0, β, ε, θ are defined in Fig. 1. In addition, $F_\odot(\lambda)$ is the spectral solar flux at heliocentric distance $d_0 = 1$ AU, r the heliocentric distance, β_π the heliocentric ecliptic latitude (i.e., measured w.r.t. the plane of symmetry Π of the zodiacal cloud). The spatial density $V(r, \beta_\pi)$ has been written as product of two independent functions:

$$V(r, \beta_\pi) = C R(r) G(\beta_\pi)$$

where C is a constant. ψ is the volume scattering function ("VSF") defined by

$$\psi(\theta, \lambda) = \frac{C}{k^2} \int_s F(\theta, \lambda, s) S(s) \, ds \quad (\mathrm{cm}^{-1}\,\mathrm{sterad}^{-1}) \quad (2)$$

and which describes the scattering properties of a unit volume of interplanetary dust.

Send offprint requests to: J.-M. Perrin

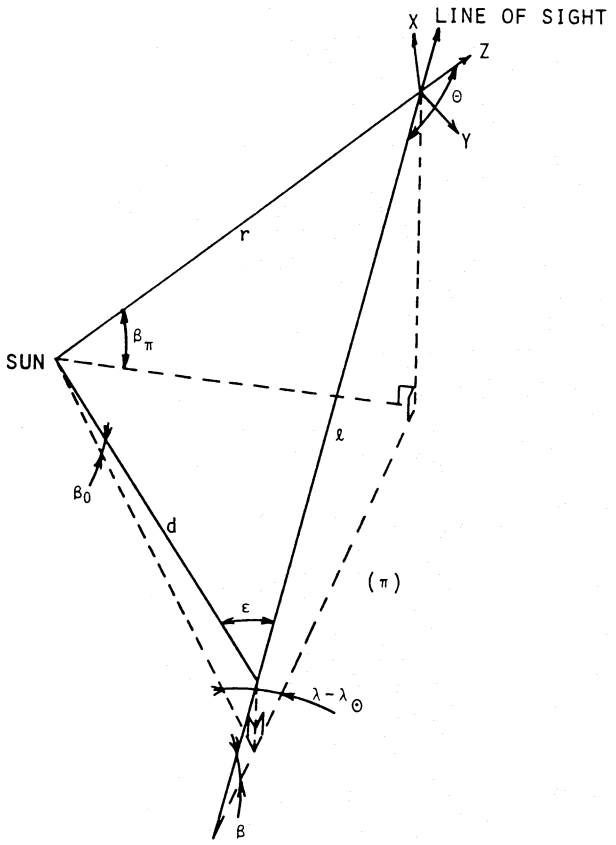

Fig. 1. Geometry and notations

In this expression $k = 2\pi/\lambda$ is the wave number of the light incident on the dust particle whose mean size is $d_s = 2s$ and whose characteristic scattering phase function is F; θ is the scattering angle. We have

$$C = N_0 \Big/ \int_s S(s)\,\mathrm{d}s$$

where N_0 is the grain number density at 1 AU and $S(s)$ is the size distribution function.

If the line of sight lies in the plane of symmetry Π and if the radial dependence of the spatial distribution R is given by

$$R(d, \varepsilon, \theta) = R(r) = r^{-\nu} = (d \sin\varepsilon/\sin\theta)^{-\nu}$$

then Eq. (1) becomes

$$Z(d, \varepsilon, \lambda) = \frac{F_\odot(\lambda)\, d_0^{\nu+2}}{(d \sin\varepsilon)^{\nu+1}} \int_\varepsilon^\Pi \psi(\theta, \lambda) \sin^\nu(\theta)\,\mathrm{d}\theta. \tag{3}$$

If the line of sight is outside the plane of symmetry but if

$$R(r) = r^{-\nu}$$

and if the angular dependence of the spatial distribution G is given by $G(\varepsilon, \beta, \beta_0, \theta) = G(\beta_\pi) = G(0)\exp(-w|\sin\beta_\pi|^u)$ then Eq. (1) becomes

$$Z(d, \beta_0, \beta, \varepsilon, \lambda) = Z(d, \beta_\pi, \varepsilon, \lambda)$$
$$= \frac{F_\odot(\lambda)\, d_0^{\nu+2}}{(d \sin\varepsilon)^{\nu+1}} \int_\varepsilon^\Pi \psi(\theta, \lambda) \sin^\nu(\theta) \exp(-w|\sin\beta_\pi|^u)\,\mathrm{d}\theta \tag{4}$$

In the case of $\beta_0 = 0$ (i.e., for an observer located in the plane Π), Lamy and Perrin (1986) have shown that, from very coherent sets of observational data of the zodiacal light and the F-corona, Eqs. (1), (3) and (4) are good models of their brightness when the spatial dust number density is given by the modified fan model

$$r^{-1}\exp(-3.5|\sin\beta_\pi|^u)$$

(i.e. when $v = 1$ and $w = 3.5$) where $u \simeq 1$ slightly increases with the ecliptic latitude β.

The color of the zodiacal light is defined w.r.t. a reference wavelength λ_0. As the color is used to obtain the physical properties of the interplanetary grains from the spectral properties of the light they scatter, solar spectral effects must be eliminated. So, following the standard definition of the color ratio at wavelength λ relative to the sun (Leinert et al., 1974), the color ratio of the zodiacal light is expressed from relationship (1) as

$$C_{ZL}(\varepsilon, \lambda, \lambda_0) = \frac{Z(d, \beta_0, \beta, \varepsilon, \lambda)/F_\odot(\lambda)}{Z(d, \beta_0, \beta, \varepsilon, \lambda_0)/F_\odot(\lambda_0)}$$
$$= \frac{\int_\varepsilon^\Pi \psi(\theta, \lambda) R(d, \varepsilon, \theta) G(\varepsilon, \beta, \beta_0, \theta)\,\mathrm{d}\theta}{\int_\varepsilon^\Pi \psi(\theta, \lambda_0) R(d, \varepsilon, \theta) G(\varepsilon, \beta, \beta_0, \theta)\,\mathrm{d}\theta} \tag{5}$$

2.2. *The color of the light scattered by dust grains*

To obtain the intrinsic properties of a dust grain from the color of the light it scatters, we use the scattering cross section σ_{sca} or the efficiency factor for scattering Q_{sca}, i.e. parameters which do not involve the directions of the incident and scattered lights. So for a grain illuminated by an incoming light of wavelength λ, the color ratio is defined by

$$C_{DG}(\lambda, \lambda_0) = \frac{\sigma_{sca}(\lambda)}{\sigma_{sca}(\lambda_0)} = \frac{Q_{sca}(\lambda)}{Q_{sca}(\lambda_0)} \tag{6}$$

with (Van de Hulst, 1957)

$$\sigma_{sca}(\lambda) = \frac{1}{k^2}\int_\wedge^{2\Pi} F(\theta, \lambda, s)\sin\theta\,\mathrm{d}\theta;$$

we note that the function F is such that

$$F(\theta, \lambda, s) = \int_0^{2\Pi} F(\theta, \varphi, \lambda, s)\,\mathrm{d}\varphi.$$

Let us consider now not only a dust grain but a set of grains whose size distribution function is $S(s)$; if we assume that there is no multiple scattering between the grains, the total scattering cross-section is defined by the expression

$$\sigma_{sca}(\lambda) = \frac{1}{k^2}\int_s \mathrm{d}s\, S(s) \int_0^{2\Pi} \mathrm{d}\varphi \int_0^\Pi F(\theta, \varphi, \lambda, s)\sin\theta\,\mathrm{d}\theta \tag{7}$$

and relationship (6) remains valid to define the color ratio of a population of dust particles. Moreover, let us suppose that the scattering function is locally axially symmetric (this is the case in the interplanetary medium for a large number of randomly oriented particles; Perrin and Lamy, 1986); then relationship (7)

becomes:

$$\sigma_{sca}(\lambda) = \frac{1}{k^2}\int_0^{\Pi} d\theta \sin\theta \int_s F(\theta, \lambda, s) S(s)\, ds$$
$$= \frac{1}{C}\int_0^{\Pi} \psi(\theta, \lambda) \sin\theta\, d\theta \quad (8)$$

2.3. Relation between the color of the zodiacal light and the color of a distribution of dust grains

We suppose thereafter that the observer is in the plan of symmetry Π.

For the model

$$V(r, \beta_\pi) \propto r^{-\nu} \exp(-w|\sin\beta_\pi|^u)$$

the color ratio of the zodiacal light defined Eq. (5) becomes

$$C_{ZL}(\varepsilon, \lambda, \lambda_0) = \frac{\int_\varepsilon^{\Pi} \psi(\theta, \lambda) \sin^\nu(\theta) \exp(-w|\sin\beta_\pi|^u)\, d\theta}{\int_\varepsilon^{\Pi} \psi(\theta, \lambda_0) \sin^\nu(\theta) \exp(-w|\sin\beta_\pi|^u)\, d\theta} \quad (9)$$

From a mathematical point of view, relationship (9) gives

$$\lim_{\varepsilon \to 0} \frac{\int_\varepsilon^{\Pi} \psi(\theta, \lambda) \sin^\nu(\theta) \exp(-w|\sin\beta_\pi|^u)\, d\theta}{\int_\varepsilon^{\Pi} \psi(\theta, \lambda_0) \sin^\nu(\theta) \exp(-w|\sin\beta_\pi|^u)\, d\theta}$$
$$= \lim_{\varepsilon \to 0} \frac{\int_\varepsilon^{\Pi} \psi(\theta, \lambda) \sin^\nu(\theta)\, d\theta}{\int_\varepsilon^{\Pi} \psi(\theta, \lambda_0) \sin^\nu(\theta)\, d\theta}$$
$$= C_{ZL}(0, \lambda, \lambda_0) \quad (10)$$

From relationships (6) and (8), the color ratio of a distribution of grains is

$$C_{DG}(\lambda, \lambda_0) = \frac{\int_0^{\Pi} \psi(\theta, \lambda) \sin\theta\, d\theta}{\int_0^{\Pi} \psi(\theta, \lambda_0) \sin\theta\, d\theta} \quad (11)$$

For the nominal model $\nu = 1$ (Lamy and Perrin, 1986), we see that

$$\lim_{\varepsilon \to 0} C_{ZL}(\varepsilon, \lambda, \lambda_0) = C_{DG}(\lambda, \lambda_0)$$

This relationship is very important since it shows that, to study the color of the zodiacal light, it is possible to separate out the influence of the elongation ε from the other mechanisms (size distribution function, spectral variation of the complex index of refraction, roughness of the surface of the grains) which can be analyzed from the spectral properties of the light scattered by a distribution of grains, i.e., the VSF. This is the subject of the following sections; in the final one, the effect of the geometrical conditions of observations (i.e., the elongation will) be taken into account.

3. Volume scattering function and size distribution

We shall consider two different functions $S(s)$ which have been recently proposed. They mostly differ by the relative importance and nature of the submicronic part of the dust population, a fact which a priori directly bears on the color of the zodiacal light. We therefore consider them as very appropriate examples for our present study.

The first size distribution function (thereafter denoted "LL") was derived by Le Sergeant d'Hendecourt and Lamy (1980) from lunar microcrater data and the "solar tracks clock" for the exposure times. The submicronic part of the population was mostly obtained from lunar sample 12 054 and the corresponding flux was subsequently found much higher than the collisional flux (Le Sergeant d'Hendecourt and Lamy, 1978, 1981). Since these authors further noted a trend of increasing bulk density of the projectiles for decreasing crater sizes, they concluded for the existence of two distinct populations: their so-called "population I" composed of grains with $s > 3\ \mu m$ and bulk densities of 2 to 3 $g\,cm^{-3}$ while their "population II" is characterized by $s < 3\ \mu m$ and larger bulk densities.

The second size distribution function (thereafter denoted "GZFG") was obtained by Grün et al. (1985). These authors have argued that

(i) while large lunar microcraters should unambiguously be attributed to interplanetary dust, craters with size below a few microns are mostly created by secondary ejecta (particularly the case of sample 12 054 because of its exposure geometry),

(ii) no lunar clock is really reliable.

They therefore derived the flux of interplanetary submicronic grains from a collisional model of the larger grains and used the results of the long-duration Pegasus impact experiment for an absolute calibration.

A comparison of the two distribution functions is illustrated in Fig. 2. A more detailed comparison with other results is presented by Grün et al. (1985). We see that the collisional flux is about two orders of magnitude smaller than the lunar flux.

The calculation of the VSF requires further assumptions concerning the optical properties of the grains as determined by their composition. The work of Grün et al. (1985) suggests that all the grains are of similar nature; we shall assume them chondritic. This will also hold for population I of the LL law. For population II, we retain a troilite (or pyrrhotite) composition suggested by the presence of "FSN" iron-sulfur-nickel particles in the collected extraterrestrial grains (Brownlee, 1978). The corresponding indices of refraction n for the selected wavelengths ranging from the ultraviolet to the red are presented in Table 1. The VSF are calculated in the radius interval [0.025–500 μm] using first Mie scattering theory; outside this interval, the contribution is negligible for all scattering angles θ larger than 2°.5. Finally, we single out the contribution of the interval [0.025–3 μm] to the VSF (i.e., population II) for both laws in order to assess and compare the role of submicronic grains. The calculated VSF are displayed in Fig. 3a, b, c, d for $\lambda = 0.22, 0.31, 0.5$ and $0.63\ \mu m$.

3.1. The LL law

Population II clearly dominates the VSF especially at scattering angles between 2°.5 and 10° where the contribution of population I is almost negligible (note that this is not true for $\theta < 2°.5$

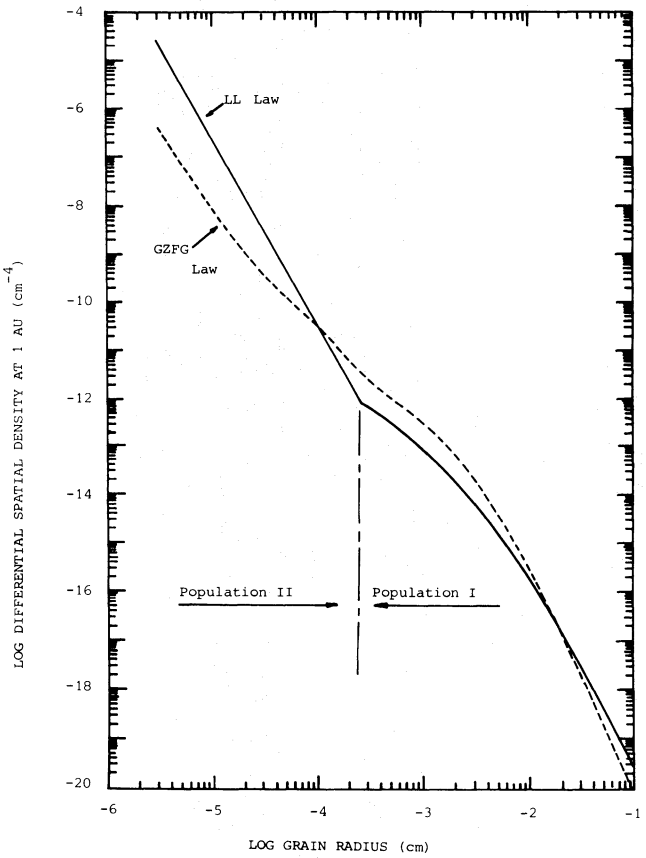

Fig. 2. Two models of the differential spatial density of interplanetary dust at 1 AU: the "LL" law (Le Sergeant d'Hendecourt and Lamy, 1980) and the "GZFG" law (Grün et al., 1985)

since diffraction by large grains will dominate); at larger angles, this contribution is small but not negligible and depends upon wavelength. It rises drastically near $\theta = 180°$ because of the "glory" effect created by dielectric spherical particles and which does not exist for the absorbing troilite grains. This strong enhancement should be viewed as somewhat artificial as it results from the assumption of sphericity inherent to Mie theory.

3.2. *The GZFG law*

The results are reversed as the contribution of population I is much larger than that of population II for all scattering angles. The "glory" effect is reinforced by the dielectric nature of the grains with $s < 3$ μm.

How do these results compare with the observed brightness of the zodiacal light. Figure 3c displays the observational VSF denoted ψ_0 recently obtained by Lamy and Perrin (1986) from an inversion of carefully selected brightness data at $\lambda = 0.5$ μm. Both laws lead to VSF in the right range but they are not really able to reproduce the shape of ψ_0 with the LL law demonstrating a slight superiority. The variation with θ is in part controlled by the assumption of smooth, spherical grains; relaxing this by the introduction of rough grains drastically improve the situation (Giese et al., 1977; Weiss-Wrana, 1983; Perrin and Lamy, 1986).

Surprisingly enough, the values of the total VSF for the two models are not drastically different. There is even a good agreement for $\theta < 70°$ in the visible and the red. For larger angles and in the ulgtraviolet, the differences are larger but never exceed a factor 2 except for the backscattering. One is further surprised when looking specifically at the influence of wavelength, i.e., color effects. There is only a moderate difference, increasing with decreasing wavelength, between the two laws but only for $\theta < 90°$; beyond, this effect is quite small. The usual view that the dominating role of submicronic particles, a situation which prevails for the LL law, would lead to a large blue enhancement (contrary to the observations) is clearly not correct. The next section attempts to clarify this situation.

4. Color, scattering theory and composition

The blue color of light scattered by particles smaller than wavelength is a consequence of the approximate expression of the efficiency factor for scattering Q_{sca} (or the cross-section σ_{sca}) in the so-called Rayleigh regime:

$$Q_{sca}(\lambda) = (\pi s^2)^{-1}\,\sigma_{sca}(\lambda) = \frac{8}{3}x^4\left|\frac{n^2-1}{n^2+2}\right|^2 \qquad (12)$$

where $x = 2\pi s/\lambda$ is the size parameter.

Clearly, assuming n constant, Q_{sca} varies with λ^{-4}, increasing rapidly as λ decreases, hence the blue color. However, n depends upon λ for real materials. Writing $n = n_r + in_i$, n_r and n_i are two real and positive functions of λ. Let us consider the sign of $\partial Q_{sca}/\partial n_i$:

$$\mathrm{sgn}\left(\frac{\partial Q_{sca}}{\partial n_i}\right) = \mathrm{sgn}\left[-n_i^4 + n_i^2(2n_r+1) + 3n_r^4 + 2n_r^2 + 2\right] \qquad (13)$$

Table 1. Optical constants of the selected materials

Wavelength	0.22 μm	0.31 μm	0.5 μm	0.63 μm
Troilite[a]	1.60+0.83i	1.42+1.16i	1.43+1.40i	1.66+1.63i
Pyrrhotite[a]	1.48+0.74i	1.37+1.23i	1.47+1.61i	1.77+1.94i
Chondrite[a,b]	1.76+0.0018i	1.91+.0022i	1.82+.0018i	1.80+.0020i
Obsidian[c,d]	1.59+0.015i	1.51+.00016i	1.48+0.000025i	1.48+0.00003i
Basalt[c,d]	1.56+0.084i	1.53+0.0017i	1.52+0.00092i	1.52+0.001i
Olivine[e]	1.82+0.025i	1.71+0.005i	1.66+0.0001i	1.66+0.0001i

References: a) Egan and Hilgeman (1979), b) Egan and Hilgeman (1975), c) Lamy (1978), d) Pollack et al. (1973), e) Huffman and Stapp (1973).

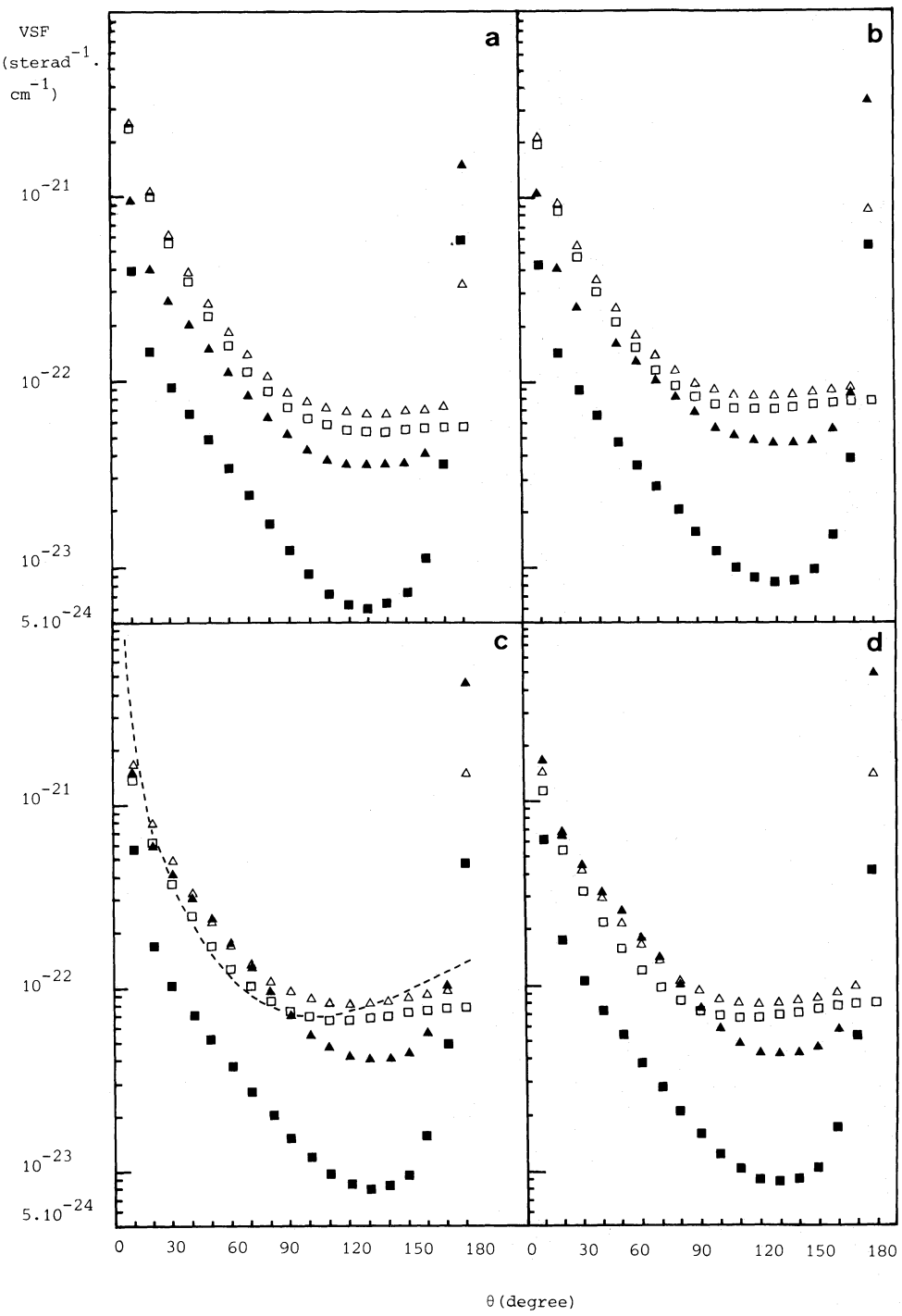

Fig. 3a–d. Calculated volume scattering functions for four wavelengths: 0.22 μm (**a**), 0.31 μm (**b**), 0.5 μm (**c**) and 0.63 μm (**d**). The open symbols correspond to the LL law and the filled symbols to the GZFG law. In addition to the total VSF corresponding to populations I + II (△, ▲), we display the contribution of the populations II (□, ■). The broken line (**c**) illustrates the VSF derived from observational results

For $n_i > 0$, the expression in the RHS of (13) has only one root n_{i0}

$$n_{i0} = \left[\frac{2n_r^2 + 1 + [(4n_r^2 + 1)^2 + 8]^{1/2}}{2}\right]^{1/2}$$

and when n_i increases from 0 to some arbitrary large value, Q_{sca} first increases, reaches its maximum value when $n_i = n_{i0}$ and then decreases. n_r is a function of λ and so is n_{i0}. However, if $n_{i0} > n_i$ and if n_i is an increasing monotonic function of λ on the spectral domain of interest D_{sp}, the equation

$$\frac{dQ_{sca}}{d\lambda} = \frac{\partial Q_{sca}}{\partial \lambda} + \frac{\partial Q_{sca}}{\partial n_i}\frac{dn_i}{d\lambda} + \frac{\partial Q_{sca}}{\partial n_r}\frac{dn_r}{d\lambda} \tag{14}$$

shows that the λ^{-4} variation of Q_{sca} (or σ_{sca}) given by the term $\frac{\partial Q_{sca}}{\partial \lambda}$ is moderated by the term $\frac{Q_{sca}}{n_i}\frac{dn_i}{d\lambda}$ which is positive and the term $\frac{\partial Q_{sca}}{\partial n_r}\frac{dn_r}{d\lambda}$ whose contribution is very small (see below).

Then, the variation of Q_{sca} is weaker than λ^{-4} therefore attenuating the blue effect. This is precisely the situation which prevails for troilite as illustrated in Fig. 4 where the color ratio

$$C_{DG}(\lambda, \lambda_0) = C_{DG}(\lambda, 0.63\ \mu m) = \frac{\sigma_{sca}(\lambda)}{\sigma_{sca}(0.63\ \mu m)} = \frac{Q_{sca}(\lambda)}{Q_{sca}(0.63\ \mu m)} \quad (15)$$

is plotted. The chondritic behaviour exhibits the opposite behaviour as n_i increases or remains constant as λ decreases and a slight reinforcement of the blue effect results (the variation of n_i with λ is not monotonic on D_{sp}).

Likewise, let us study the sign of $\partial Q_{sca}/\partial n_r$; it is governed by the equation

$$n_r^4 + n_r^2(1-2n_i)^2 - 3n_i^4 + n_i^2 - 2 = 0$$

which has only one root n_{r0} for $n_r > 0$

$$n_{r0} = \left[\frac{2n_i^2 - 1 + [(4n_i^2-1)^2+8]^{1/2}}{2}\right]^{1/2}$$

When n_r increases from 0 to some arbitrary large value, Q_{sca} first decreases, reaches its minimum value when $n_r = n_{r0}$ and then increases. n_{r0} is a function of λ via n_i. However, if $n_{r0} > n_r$ and if n_r is a monotone decreasing function of λ on D_{sp}, then Q_{sca} decreases with λ more steeply than the λ^{-4} variation. Practically, the variations of n_r on D_{sp} are much less than those of n_i and the spectral behaviour of n_r has a limited influence on Q_{sca}. This is almost negligible for the materials considered here.

Figure 4 shows that, despite its reduction, the blue color of the light scattered by small grains of troilite in the Rayleigh approximation is a sufficiently large effect which would clearly appear in the zodiacal light. Let us now go one step further and use the more rigourous Mie theory to calculate Q_{sca} integrated over the size distribution function of population II of the LL law. The blue color is drastically reduced as illustrated in Fig. 4, even in the case of a chondritic composition. We have considered additional materials and found that olivine, basalt and obsidian lead to results very similar to chondrite while pyrrhotite has even a more neutral color then troilite.

The fact that the applicability of the Rayleigh approximation is severely limited has already been discussed by us (Perrin and Lamy, 1981): further to the condition $s \ll \lambda$, it requires that the complex part of the refractive index n_i is not too large. This second condition is clearly violated in the ultraviolet by all materials considered here, even by the "dielectric" silicates which become true absorbers in this spectral domain.

In this framework, we understand the results of Grün et al. (1985) who calculated Q_{sca} for various materials (obsidian, basalt, olivine) and wavelengths to rule out a distribution favoring small grains. Further to the fact that the effect of the size distribution was not introduced, the selected materials have the same common characteristic, namely that the imaginary part of their index of refraction decreases with wavelength resulting in an enhanced blue effect in the ultraviolet.

5. Color and rough particles

The problem of light scattering by rough particles is complex. When the size of the particles is much larger than the wavelength of the incident light, experimental results (see, for example, Giese et al., 1977; Weiss-Wrana, 1983) have shown large and systematic differences w.r.t. the results from Mie theory. In a preliminary

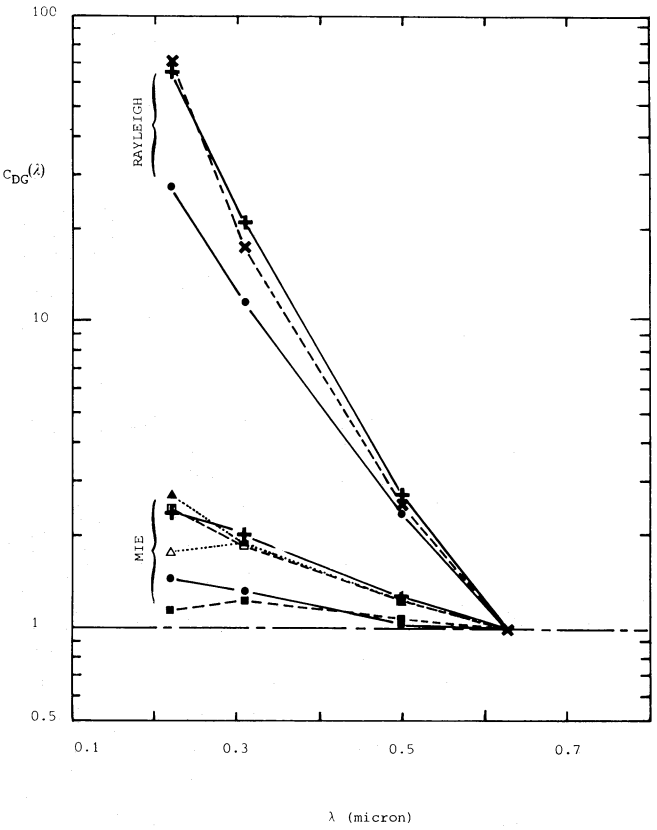

Fig. 4. The color of the scattered light (normalized at 0.63 μm) for the population II of the LL law as obtained from the Rayleigh approximation and the Mie theory and for various materials: chondrite (+), troilite (●) olivine (□), basalt (△), obsidian (▲), pyrrhotite (■) and an artificial material having a constant index of refraction (×)

effort to interpret those results, Giese et al. (1977) have hinted that several independent scattering processes are taking place: forward diffraction, Fresnel reflection, non-polarized reflection and transmission. Various models have been proposed for each of these processes (see, for example, Perrin and Lamy, 1986 for a review). Experimental comparisons led Geake et al. (1984) to retain the approach proposed by Wolff (1975, 1980, 1981) for the two last processes: it considers single and double reflections by a rough surface as well as non-polarized transmission. Taking into account the effects of the curvature of the particles with the resulting shadowing, we have obtained a vectorial description at the light scattered by a rough particle outside the neighbourhood of the forward direction (Perrin and Lamy, 1983). For the forward scattering, we used the high energy approximation (H.E.A.) whose first phenomenological adaption to rough particle was made by Chiappetta (1980). Briefly this method can be introduced by comparison with classical electrodynamic; following this theory, a component φ of the electromagnetic field scattered by a spherical particle of complex index of refraction n, is classically obtained from the Helmoltz equation:

$$\nabla^2 \varphi(\boldsymbol{r}) + n^2 k^2 \varphi(\boldsymbol{r}) = 0 \quad (16)$$

whose solution at a point $\boldsymbol{r}$ far away from the particle is given by

$$\varphi(\boldsymbol{r}) = \exp(i\boldsymbol{kr}) + f(\theta)\exp(ikr)/r \quad (17)$$

where $r = |\boldsymbol{r}|$. The first term represents the incident wave and $f(\theta)$, the amplitude of the scattered wave whose expression is

$$f(\theta) = -\frac{k^2}{4\Pi}\int_{\mathscr{V}} \exp(-\frac{k}{r}\boldsymbol{r}\boldsymbol{r}')(1-n^2)\,\varphi(\boldsymbol{r}')\,\mathrm{d}r' \qquad (18)$$

where $\mathscr{V}$ is the volume of the sphere.

These equations are similarly to those obtained in the Schrödinger formalism where the interaction of wave with an arbitrary particle may be investigated in the framework of the interaction of a wave with a scattering potential V. The wave function $\varphi(\boldsymbol{r})$ satisfies the Schrödinger equation

$$\nabla^2\varphi(\boldsymbol{r}) + k^2(1 - V(\boldsymbol{r})/E)\,\varphi(\boldsymbol{r}) = 0 \qquad (19)$$

where E is the energy of the incident wave. The solutions are given by expressions like (17) and (18) but where $(1-n^2)$ is replaced by $V(r)/E$. The equality $V = (1-n^2)E$, valid in the case of a sphere, still hold for a rough particle but the index of refraction is modified, for instance by introducing a distribution of the Fermi type (Chiappetta, 1980). The H.E.A. gives an approximate expression of the amplitude of the scattered waves valid only in the neighbourhood of the forward direction. A most elaborated form, valid for all value of the scattering angle, have been obtained by Perrin and Lamy (1986). However, this involves a triple integral (over the impact parameter, the radius s and the scattering angle θ) for each value of wavelength and of the parameters describing the roughness. The simpler scalar description obtained in the high-energy approximation (Perrin and Chiappetta, 1985) which requires only the mean amplitude of the roughness – and not the effective angles for simple and double reflections – is ample for the present study. Let us consider the case where the mean amplitude of roughness d_r is proportional to the mean radius, viz

$$d_r = c_d s \qquad c_d \in [0.01, 0.25]$$

and apply our model to the dominating population I (the condition $s \gg \lambda$ is required) of the GZFG law to illustrate the role of roughness on color (the Mie theory being still used for population II). Figure 5 gives the color ratio

$$C_{DG}(\lambda, 0.63) = \sigma_{sca}(\lambda)/\sigma_{sca}(0.63\ \mu\mathrm{m})$$

for different values of the roughness parameter c_d and further illustrates the overwhelming role of population I in controlling the color. But the most interesting result is the change of color with c_d, from the blue for large values of the roughness, to neutral and to the red for smaller and smaller values. Several studies of the color of the light scattered by rough surfaces performed by Egan and Hilgeman (1978) generalizing the work of Aronson and Emslie (1973) and by Schiffer (1985) has already shown that a roughness with an amplitude smaller than wavelength leads to a reddening of the scattered light. Our analysis, based on an entirely different approach, confirms these conclusions for the case of large, rough spheres and further shows an opposite trend when the roughness becomes large.

This can be understood by comparing the mean amplitude of the roughness with the wavelength of the incident light: it appears larger for ultraviolet radiations than for visible one. So, for an amplitude much larger than the interaction wavelengths the scattering intensity in the neighbourhood of the forward direction and the enhancement for scattering angles larger than 90° are more pronounced for shorter wavelengths than for the larger ones. But when the mean amplitude of the roughnesses is smaller than or of the same order as the wavelength, diffuse phenomenae are less important for small wavelengths than for larger ones and the opposite result takes place.

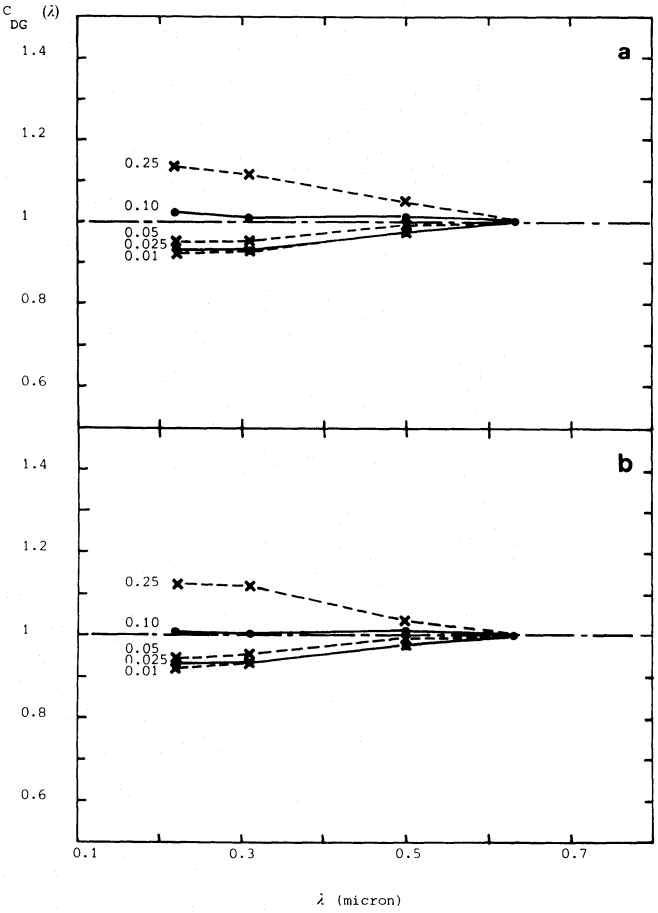

Fig. 5a and b. The color of the scattered light (normalized at 0.63 μm) for the GZFG law and for various values of the roughness parameters C_d ranging from 0.01 to 0.25: population II alone (**a**) and global results, i.e., populations I + II (**b**).

6. Color and elongation

To deduce the properties of the interplanetary dust from the color of the zodiacal light, it is necessary to compare its color ratio with the color ratio of a set of dust particles having the same size distribution. We have obtained (Sect. 2)

$$C_{DG}(\lambda, \lambda_0) = C_{ZL}(\varepsilon = 0, \lambda, \lambda_0)$$

Then for any line-of-sight of elongation ε, the color of the zodiacal light $C_{ZL}(\varepsilon, \lambda, \lambda_0)$ can be deduced form $C_{DG}(\lambda, \lambda_0)$ if the contribution of the angular domain $[0, \varepsilon]$ to the value of $C_{DG}(\lambda, \lambda_0)$ is known. Letting aside the spectral variation of the index of refraction, this contribution does vary with wavelength: it increases with decreasing wavelength (as seen above, this is particularly the case for large rough particles but holds also for small spheres). Recalling that

$$C_{DG}(\lambda, \lambda_0) = \frac{\sigma_{sca}(\lambda)}{\sigma_{sca}(\lambda_0)}$$

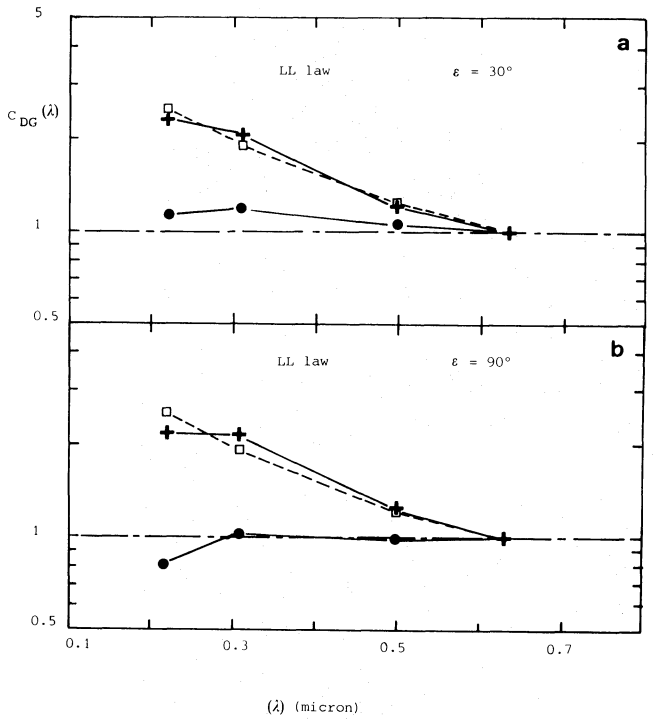

Fig. 6a and b. The color of the scattered light (normalized at 0.63 μm) for the LL law at two elongations: $\varepsilon = 30°$ (**a**) and $\varepsilon = 90°$ (**b**) and for three materials: olivine (□), chondrite (+) and troilite (●)

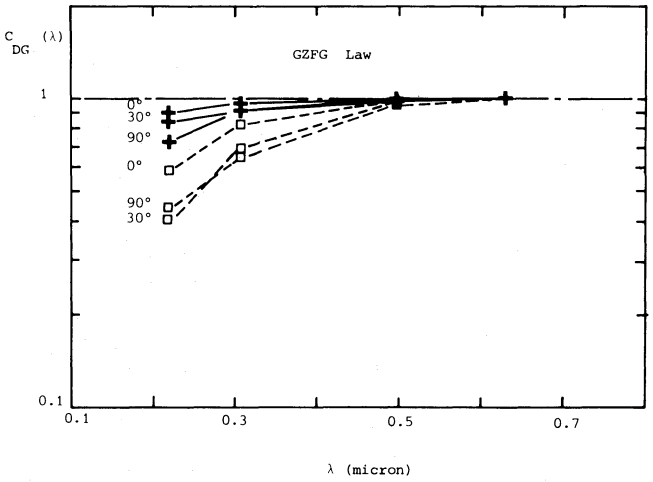

Fig. 7. The color of the scattered light (normalized at 0.63 μm) for the GZFG law at elongations (0°, 30° and 90°) and for two materials: olivine (□) and chondrite (+)

and noting that, for $\lambda < \lambda_0$, the contribution of the interval $[0, \varepsilon]$ is larger for $\sigma_{sca}(\lambda)$ than for $\sigma_{sca}(\lambda_0)$ up to a value ε_B, we find that $C_{DG} > C_{ZL}$ (ε_B depends upon the physical parameters of the grains, composition, roughness, and is typically between 15° and 30°) (Giese et al., 1977; Weiss-Wrana, 1983). Therefore, the geometrical conditions of the observations reduce any intrinsic blue effect (and possibly introduce a reddening): "the observations redden the results". This is illustrated in the case of the smaller dust particles (population II) of the LL law by a comparison of Fig. 4, which corresponds to $\varepsilon = 0$ and Fig. 6a which corresponds to $\varepsilon = 30°$. When $\varepsilon > \varepsilon_B$, the decrease in function of F diminishes (F may even increase for $\varepsilon > 90°$) and is offset by the increase of the factor λ^2 [Eq. (7)]: either the above behaviour still holds as shown by a comparison of Fig. 6a ($\varepsilon = 30°$) and Fig. 6b ($\varepsilon = 90°$) or is reversed as illustrated for the GZFG law in Fig. 7.

The comparison of observational results obtained by different authors faces various problems such as instrumental calibrations and background subtraction, particularly acute in the ultraviolet, resulting sometime in discrepancies or even contradictions. The influence of the elongation on the color of the zodiacal light is best assessed by comparing results obtained by the same instrument at different elongations. Cebula and Feldman (1982) observed the zodiacal light in the ultraviolet at $\varepsilon = 21°.2$ and $29°.5$ and concluded that the reddening increases with ε in this interval, although the error bars are large. This is precisely the behaviour we obtained in the case $\varepsilon < \varepsilon_B$. From the Helios *UBV* observations, Leinert et al. (1982) found that the reddening slightly decreases with increasing elongation, but this effect is really perceptible for $\varepsilon > 90°$ owing to the accuracy of the measurements. This corresponds to one of the situations we described above for $\varepsilon > \varepsilon_B$.

Although the very observation of the zodiacal light as a function of elongation introduces an intrinsec color effect, one should not forget the influence of the possible heterogeneity of the interplanetary dust cloud (size, composition, roughness) which may reinforce or attenuate the above effect.

7. Conclusion

We see that the color of the zodiacal light and more generally, the color of the light scattered by a cloud of dust particles is a complex phenomenon governed by many different factors. We have studied in this work the influence of several of these factors, size distribution function, spectral variation of the complex index of refraction and roughness of the particles. A particular example based on two different size distribution functions shows that they lead to rather similar volume scattering functions and further to not drastically different color although the two distributions differ very much in their proportions of submicronic grains. The very geometry for observing the zodiacal cloud implies also a color effect since only partial scattering cross-sections (limited to the elongation ε) are retrieved. We note that the separation of the geometrical factors is rendered particularly simple by the model $\nu = 1$, a value justified by our own study (Lamy and Perrin, 1986) at least for the inner zodiacal light. A value $\nu \neq 1$ would make relationship (10) more complex but the variations of C_{DG} and C_{LZ} would go in the same direction. We have not considered the color effect of an inhomogeneous cloud; although there are growing evidences for the variation of the physical properties of the grains with heliocentric distance (Lamy and Perrin, 1986; Hong and Um, 1987), this is not yet sufficiently characterized for being modelled. But we may suspect that such a variation will bear on the color as well. All this shows how difficult it is to interpret the color of the zodiacal light.

References

Aronson, J.R., Emslie, A.G.: 1973, *Appl. Opt.* **12**, 1223

Brownlee, D.E.: 1978, in *Cosmic Dust*, ed. J.A.M. McDonnell, Wiley, Chichester, New York, Brisbane, Toronto, p. 295

Cebula, R.P., Feldman, F.D.: 1982, *Astrophy. J.* **263**, 987

Chiappetta, P.: 1980, *Astron. Astorphys.* **83**, 348

Dumont, R.: 1973, *Planetary Space Sci.* **21**, 513

Dumont, R., Sanchez, F.: 1975, *Astron. Astrophys.* **38**, 405

Egan, W.G., Hilgeman, T.: 1975, *Astron. J.* **80**, 587

Egan, W.G., Hilgeman, T.: 1978, *Appl. Opt.* **17**, 245

Egan, W.G., Hilgeman, T.: 1979, *Optical Properties of Inhomogeneous Materials*, Academic Press, New York, San Fransisco, London

Geake, J.E., Geake, M., Zellner, B.H.: 1984, *Monthly Notices Roy. Astron. Soc.* **210**, 89

Giese, R.H., Weiss, K., Zerull, R.H., Ono, T.: 1977, *Astron. Astrophys.* **65**, 777

Grün, E., Zook, H.A., Fechtig, H., Giese, R.H.: 1985, *Icarus* **62**, 244

Hong, S.S., Um, I.K.: 1987, *Astrophys. J.* **320**, 928

Huffman, D.R., Stapp, J.L.: 1973, in *Interstellar Dust and Related Topics*, eds. M. Greenberg, H.C. Van de Hulst, p. 297

Lamy, P.L.: 1978, *Icarus* **34**, 68

Lamy, P.L., Perrin, J.-M.: 1986, *Astron. Astrophys.* **163**, 269

Leinert, C., Link, H., Pitz, E.: 1974, *Astron. Astrophys.* **30**, 411

Leinert, C., Richter, I., Pitz, E., Hanner, M.: 1982, *Astron. Astrophys.* **110**, 355

Le Sergeant d'Hendecourt, J.B., Lamy, P.L.: 1978, *Nature* **276**, 800

Le Sergeant d'Hendecourt, J.B., Lamy, P.L.: 1980, *Icarus* **43**, 350

Le Sergeant d'Hendecourt, J.B., Lamy, P.L.: 1981, *Icarus* **47**, 270

Perrin, J.-M., Chiappetta, P.: 1985, *Opt. Acta* **32**, 907

Perrin, J.-M., Lamy, P.L.: 1981, *Opt. Acta* **28**, 595

Perrin, J.-M., Lamy, P.L.: 1983, *Opt. Acta* **30**, 1223

Perrin, J.-M., Lamy, P.L.: 1986, *Opt. Acta* **33**, 1001

Pollack, J.B., Toon, O.B., Khare, B.N.: 1973, *Icarus* **19**, 372

Schiffer, R.: 1985, *Astron. Astrophys.* **148**, 347

Van de Hulst, H.C.: 1957, *Light Scattering by Small Particles*, Wiley, New York

Weiss-Wrana, K.: 1983, *Astron. Astrophys.* **126**, 240

Wolff, M.: 1975, *Appl. Optics* **14**, 1395

Wolff, M.: 1980, *Icarus* **44**, 780

Wolff, M.: 1981, *Appl. Optics* **20**, 2493